

## First-principles study of the electronic structure of heavy fermion $\text{YbRh}_2\text{Si}_2$

This article has been downloaded from IOPscience. Please scroll down to see the full text article.

2006 J. Phys.: Condens. Matter 18 6289

(<http://iopscience.iop.org/0953-8984/18/27/012>)

View [the table of contents for this issue](#), or go to the [journal homepage](#) for more

Download details:

IP Address: 129.252.86.83

The article was downloaded on 28/05/2010 at 12:15

Please note that [terms and conditions apply](#).

# First-principles study of the electronic structure of heavy fermion $\text{YbRh}_2\text{Si}_2$

T Jeong<sup>1</sup> and W E Pickett<sup>2</sup>

<sup>1</sup> DPMC, University of Geneva, 24 Quai Ernest-Ansermet, CH-1211 Geneva 4, Switzerland

<sup>2</sup> Department of Physics, University of California, Davis, CA 95616, USA

Received 2 May 2006

Published 23 June 2006

Online at [stacks.iop.org/JPhysCM/18/6289](http://stacks.iop.org/JPhysCM/18/6289)

## Abstract

The electronic properties of  $\text{YbRh}_2\text{Si}_2$  are studied by means of band structure calculations based on the density functional theory within the LDA (local density approximation), LDA +  $U$ , and fully relativistic scheme. The 4f derived bands are studied within a relativistic framework which yields flat and spin-orbit split bands, and a correlated band method (LDA +  $U$ ) that includes correlation corrections. In both cases the uppermost 4f band is located roughly 150 meV below the Fermi energy  $E_F$ , and hybridizes weakly with the dispersive Rh 4d bands and a Rh 4d<sub>xy</sub> band that does not disperse perpendicular to the Rh layers. When we applied the fully relativistic scheme, the 4f derived bands split into  $j = 7/2$  and  $5/2$  excitations due to spin-orbit coupling effects. The  $f_{7/2}$  multiplet is located much closer to  $E_F$ , hybridizing anisotropically with a Rh 4d derived conduction band. This mixing induces a non-integer occupation of the f levels  $n_f$  and hence reveals that  $\text{YbRh}_2\text{Si}_2$  is a mixed-valence heavy fermion. The 4f electrons can be delocalized through the hybridization with conduction electrons. And the hybridization between f and conduction d electrons plays a important role in  $\text{YbRh}_2\text{Si}_2$ . The Fermi surface splits into three different non-touching sheets. There are two tiny cylinder Fermi surfaces around Z points which are from the Rh 4d bands and the larger Fermi surfaces are from the 4f derived bands.

(Some figures in this article are in colour only in the electronic version)

## 1. Introduction

The strongly correlated electron systems has been attractive in condensed matter physics in recent years, in particular heavy fermion (HF) metals which are close to a magnetic quantum critical point (QCP). This is due to the fact that such systems develop low temperature thermodynamic, transport and magnetic properties that deviate from the conventional Landau Fermi liquid (LFL) theory. The most interesting feature is that the ground state properties can be tuned around a magnetic QCP by a control parameter such as pressure, magnetic field or

doping [1]. At present, an increasing number of examples of Ce and U based systems such as  $\text{CeCu}_{6-x}$ ,  $\text{CePd}_2\text{Si}_2$  and  $\text{CeIn}_3$  have been found to exhibit magnetic quantum criticality by either doping tuning or pressure tuning [2–4]. Heavy fermions are characterized by a large effective quasiparticle mass as reflected in the strongly enhanced electronic specific heat coefficient and spin susceptibility at low temperature. Among these,  $\text{YbRh}_2\text{Si}_2$  has attracted attention as the first observed Yb based HF system that is located in the vicinity of the QCP and exhibits a non-Fermi liquid (NFL) behaviour at ambient pressure.

The heavy fermion  $\text{YbRh}_2\text{Si}_2$  lies very close to a magnetic instability, related to the disappearance of antiferromagnetic (AFM) order. The AFM ground state has a very tiny value of the ordered magnetic moment of  $\mu_{\text{Yb}} \approx (10^{-2}-10^{-3}) \mu_{\text{B}}$  as reported from muon spin relaxation ( $\mu\text{SR}$ ) measurements [5] at ambient pressure below the Néel temperature  $T_{\text{N}} \simeq 70$  mK. This is one of the lowest magnetic ordering temperatures observed in strongly correlated electron systems. At  $T > T_{\text{N}}$  pronounced deviations from the Landau Fermi liquid behaviour are observed up to temperatures of 10 K [6, 7]. A tiny magnetic field of  $B_{\text{c}} = 0.06$  T is sufficient to suppress the weak AFM order leading to a field-induced QCP. Therefore  $\text{YbRh}_2\text{Si}_2$  is a favourable compound for investigating NFL phenomena which are related to the proximity of a QCP. The resistivity  $\rho$  and electronic specific heat  $\Delta C$  at low  $T$  show  $\Delta\rho = \rho - \rho_0 \propto T$  and  $\Delta C/T \propto -\ln T$ , respectively, which is characteristic of NFL behaviour [6]. This behaviour contrasts with the conventional Landau Fermi liquid (LFL) behaviour of  $\Delta\rho \propto T^2$  and  $\Delta C/T = \text{const}$ . An external pressure compresses the atomic lattice leading to an increase of the antiferromagnetic coupling ( $p \leq 2.7$  GPa,  $T_{\text{N}} \approx 1$  K at 2.7 GPa) [6, 8], as opposed to expanding the lattice by replacing Si by Ge [9] or Yb by La which enhances the Kondo coupling and reduces  $T_{\text{N}}$ . Approximately 5% Ge or La doping completely destroys the antiferromagnetic order in  $\text{YbRh}_2\text{Si}_2$ . The existence of spin fluctuations in this low moment state has been reported from low temperature  $\text{Si}^{29}$  NMR and  $\mu\text{SR}$  experiments on  $\text{YbRh}_2\text{Si}_2$  [5, 10].

Norman reported energy band studies with the LMTO code recently [11]. Since this band structure was calculated within the local density approximation (LDA) scheme, further studies, such as ones using LDA +  $U$ , the fully relativistic scheme for the spin–orbit coupling effects, are required. In this work we study and compare the electronic structures of  $\text{YbRh}_2\text{Si}_2$  with the LDA, LDA +  $U$ , and the fully relativistic method based on the density functional theory.

## 2. Crystal structure

$\text{YbRh}_2\text{Si}_2$  belongs to the  $\text{ThCr}_2\text{Si}_2$ -type tetragonal crystal structure ( $I4/mmm$  space group, 139) with Yb occupying the 2a site ( $4/mmm$  site symmetry), Rh the 4d site ( $4m2$ ) and Si the 4e site ( $4mm$ ). In figure 1 the crystal structure of  $\text{YbRh}_2\text{Si}_2$  is shown. Since the major contributions to  $N(E_{\text{F}})$  come from Yb and Rh, the local environment of Yb and Rh atoms is particularly important for our concerns. As you can see, the Yb atom lies on a bct sublattice and Rh atoms lie on a simple tetragonal sublattice rotated by  $45^\circ$  in the plane. The Yb–Rh distance is 3.17 Å and the Si–Si distance is 2.46 Å. We used the experimental lattice constants  $a = 4.010$  Å and  $c = 9.841$  Å [6].

## 3. Method of calculations

We have applied the full potential nonorthogonal local orbital minimum basis (FPLO) scheme within the local density approximation (LDA) [12]. In these scalar relativistic calculations we used the exchange and correlation potential of Perdew and Wang [13]. Yb 4s, 4p, 4d, 4f, 5s, 5p, Rh 4s, 4p and Si 2s, 2p states were included as valence states. All lower states were

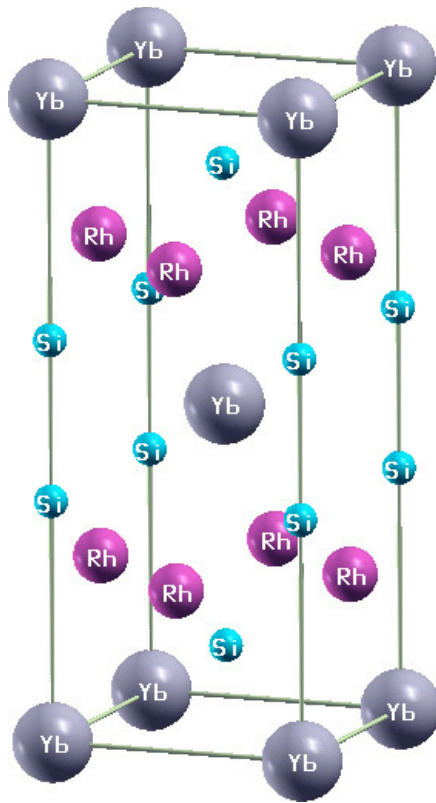


**Figure 1.** The tetragonal crystal structure of  $\text{YbRh}_2\text{Si}_2$ . The largest atoms are Yb, the middle size atoms are Rh and the smallest ones are Si.

treated as core states. We included the relatively extended semicore 4s, 4p, 4d, 4f states of Yb as band states because of the considerable overlap of these states on nearest neighbours. This overlap would be otherwise neglected in our FPLO scheme. Yb 6p states were added to increase the quality of the basis set. The spatial extension of the basis orbitals, controlled by a confining potential  $(r/r_0)^4$ , was optimized to minimize the total energy. The self-consistent potentials were obtained on a  $k$  mesh of 24  $k$  points in each direction of the Brillouin zone, which corresponds to 1063  $k$  points in the irreducible zone.

#### 4. Results

We first discuss the band structure results from the conventional theoretical methods in the local density approximation. The full band structure of  $\text{YbRh}_2\text{Si}_2$  is shown in figure 2, which is very similar to that for Norman's calculation. The Si 3s states lie between  $-11$  and  $-8$  eV; above them there are Rh 4d–Si 3p hybrids in the range of  $-6.5$  to  $+1$  eV. Centred  $0.25$  eV below the Fermi level with a width of  $0.1$  eV are the very flat Yb 4f bands, hybridized with the other bands at crossings. Above the Fermi energy there are varying amounts of Yb 6s, 5d, Rh 5s, Si 3s, 3p states. A prominent feature of the band structure near  $E_F$ , besides the 4f bands, is the Rh  $d_{xy}$  (in-plane) character. A band with primarily this character lies  $30$  meV below  $E_F$ , is completely flat along  $\Gamma$ –Z (no  $k_z$  dispersion) and disperses upward in the  $k_x, k_y$  plane giving rise to a tiny

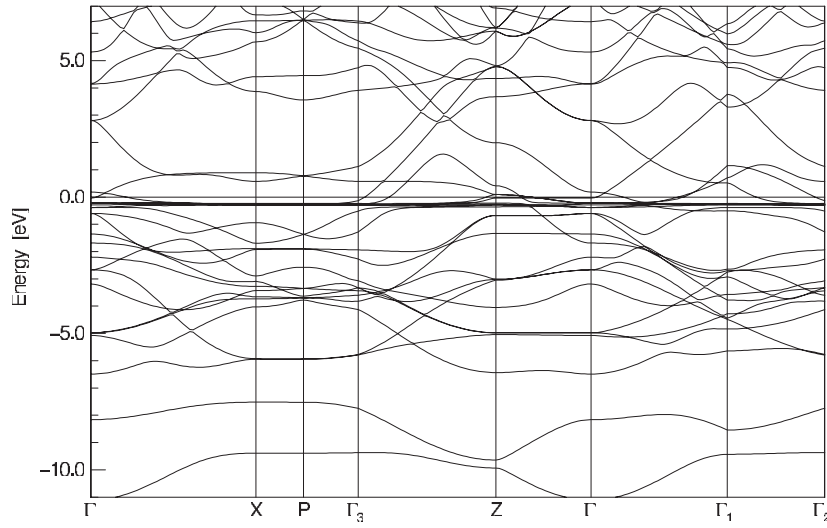


**Figure 2.** The full band structures of YbRh<sub>2</sub>Si<sub>2</sub> along symmetry lines. The symmetry line indices are  $\Gamma$  (0, 0, 0), X (0.5, 0.5, 0), P (0.5, 0.5, 0.204),  $\Gamma_3$  (0.417, 0.417, 0.407), Z (0, 0, 0.407),  $\Gamma_1$  (0, 0.583, 0),  $\Gamma_2$  (0.417, 0.583, 0).

cylinder Fermi surface surrounding the  $\Gamma$ -Z line ( $k_x = 0 = k_y$  line). Even given that this is a  $d_{xy}$  band, it is remarkable that there is so little  $k_z$  dispersion. There is also substantial Rh  $4d_{xy}$  character 5–6 eV below  $E_F$  and again a flat band around  $-5$  eV, from which it is evident that the two Rh  $4d_{xy}$  states form a bonding pair at  $-5$  eV and an antibonding pair very near  $E_F$  (at  $k_x = 0 = k_y$ ). A band that is Yb  $4d_{x^2-y^2}$  at  $\Gamma$ , 0.18 eV above  $E_F$  disperses downward across the Fermi level and crosses the 4f bands, and transforms into Rh 4d character. Thus while the  $d_{x^2-y^2}$  orbital also lies in the  $x$ - $y$  plane, it is only the  $4d_{xy}$  state that has no  $k_z$  character. Other bands of more mixed Rh + Si character also disperse through the Fermi level.

We also study the on-site atomic-like correlation effects beyond LDA by using the LDA +  $U$  approach in a rotationally invariant, full potential implementation [14]. Minimizing the LDA +  $U$  total energy functional with spin-orbit coupling (SOC) treated self-consistently [15] generates not only the ground state energy and spin densities, but also effective one-electron states and energies that provide the orbital contribution to the moment and Fermi surfaces. The basic difference of LDA +  $U$  calculations from the LDA is the explicit dependence on the on-site spin and orbitally resolved occupation matrices. The Coulomb potential  $U$  and the exchange coupling  $J$  for the Ce 4f orbitals have been chosen to be 7.5 and 0.68 eV respectively. The band structure calculated within the LDA +  $U$  scheme is shown in the middle panel of figure 3. We observe that the crystal field splittings of Ce 4f bands within LDA are quite small and in fact difficult to identify due to hybridization with itinerant bands. From LDA +  $U$ , the 4f bands are still very flat but are split (in a 1–3–3 fashion from the bottom up) by some combination of the crystal field and the anisotropy of the  $U$  interaction by a total 1.6 eV. The upper 4f band is located at  $-0.1$  eV; this is of  $4f_{z(x^2+y^2)}$  character. This 4f orbital has the same shape as the  $4f_{xyz}$  orbital, but is rotated around the  $z$ -axis so its lobes lie in the  $x$ - $z$  and  $y$ - $z$  planes. These lobes point almost directly at the Rh sites, and as a result this orbital mixes with the Rh  $4d_{xy}$  flat band along  $\Gamma$ -Z. However, this 4f orbital mixes more strongly with the dispersing Rh  $5d_{xz}$ ,  $5d_{yz}$  band near the  $\Gamma$  and  $\Gamma_1$  points. This latter mixing occurs through a  $t_{df\sigma}$  tight binding hopping amplitude; mixing with the flat  $4d_{xy}$  band occurs through a combination of  $t_{df\sigma}$  and

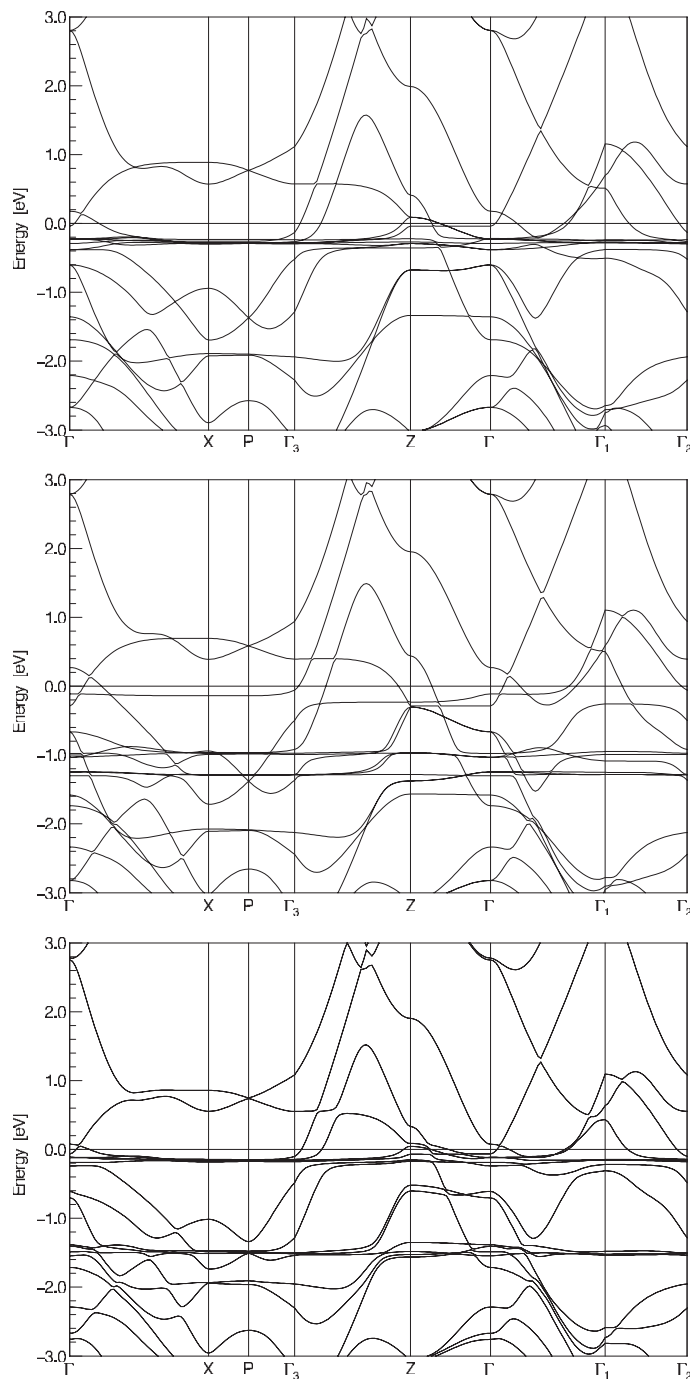


**Figure 3.** Top panel: the blow-up LDA band structure of  $\text{YbRh}_2\text{Si}_2$ . There is one totally flat band within 50 meV of Fermi level due to the Rh  $d_{xy}$  along  $Z$ - $\Gamma$  symmetry line. Middle panel: the LDA +  $U$  scheme band structure of  $\text{YbRh}_2\text{Si}_2$ . Bottom panel: the fully relativistic band structure of  $\text{YbRh}_2\text{Si}_2$  near the Fermi level. We can see the Yb 4f splitting due to the spin-orbit coupling. The splitting is about 1.3 eV.

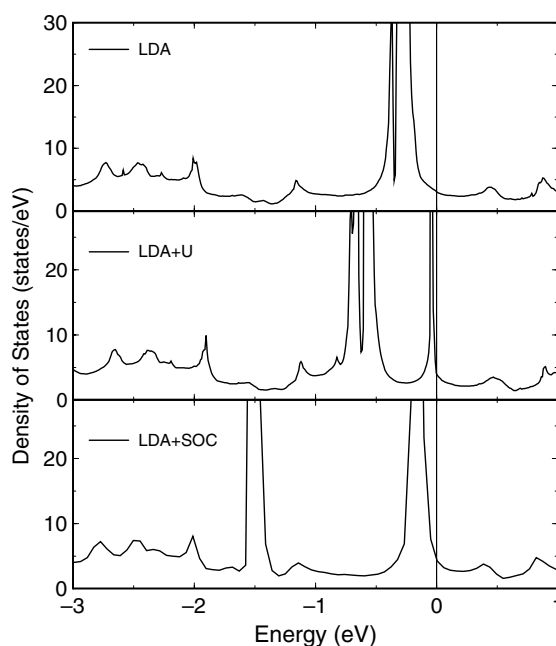


**Figure 4.** The density of states of  $\text{YbRh}_2\text{Si}_2$ . Top panel: DOS of LDA; the Yb 4f bands dominate the states near the Fermi level. Middle panel: DOS of LDA +  $U$ ; the 4f bands has 1–3–3 bands splits. Bottom panel: showing the spin–orbit coupling effects of the fully relativistic calculation. The splitting is about 1.3 eV.

$t_{df\pi}$  hoppings. The LDA 4f derived bands have a small crystal field splitting which is enhanced by LDA +  $U$  into the three manifolds (1–3–3) as in the LDA case, but too small to show up. The tetragonal distortion is small and so the splitting is due to the bcc symmetry [16].

We also calculated the fully relativistic band structure to see the spin–orbit coupling effects. The result is shown in the bottom panel of figure 3. As you can see, the spin–orbit interaction splits the 4f states into two manifolds, located 0.15 and 1.5 eV below the Fermi level, the  $4f_{7/2}$  and the  $4f_{5/2}$  multiplet respectively. Since the  $4f_{7/2}$  levels lie nearer  $E_F$  than in LDA, there will be more 4f character on the Fermi surface. The 4f states hybridize at crossings with the Rh 4d bands, but elsewhere are very flat. The corresponding total electronic density of states with two strong peaks comes from the 4f states.

Densities of states for the LDA, LDA +  $U$  and fully relativistic calculation are shown in figure 4. Near the Fermi level the main contribution is the Yb 4f states with some mix of Rh 4d states. The very flat Yb f band makes a high peak in the density of states 0.25 eV below the Fermi level in the LDA calculation. We can observe the 1–3–3 splitting in the LDA +  $U$  calculation and two manifolds in the fully relativistic scheme. We obtain the number of states at the Fermi level  $N(E_F)$  of  $3.10 \text{ eV}^{-1}$  per formula unit basis for the LDA calculation,  $3.98 \text{ eV}^{-1}$  for the LDA +  $U$  and  $4.28 \text{ eV}^{-1}$  for the fully relativistic calculation.

The question remains: which band structure (LDA, LDA +  $U$  or LDA + SOC) is more realistic? In LDA + SOC (the fully relativistic scheme), SOC is applied at the one-electron level, that is, each 4f orbital acquires its own  $j = l \pm s$  ( $\frac{7}{2}$  or  $\frac{5}{2}$ ) label and character. In LDA +  $U$ , one can follow Hund’s rules to some extent: maximize  $S = \sum_i s_i$  and maximize  $L = \sum_i l_i$ , and study various values of  $J$  (or even of  $L$ ). In some respects, such as for the ground state energy for determining the equation of state, the LDA +  $U$  approach seems most appropriate

for rare earth ions. There are several instances of experience with similar 4f configurations which imply that the LDA +  $U$  correction is essential; simple LDA often leaves occupied 4f states at too high an energy and unoccupied ones at too low an energy, so there is excessive hybridization at the Fermi level. One example is that of Gd metal [17]; another is provided by the Eu mononpnictides [18]. On the other hand, 4f single-particle-like excitations are likely to be characterized by the  $\frac{7}{2}, \frac{5}{2}$  labels. The excitations  $f^0 \rightarrow f^1$  or  $f^{14} \rightarrow f^{13}$  are likely to show SOC aspects directly. Fisk *et al* did an angle-resolved photoemission spectroscopy experiment which is a powerful technique for directly probing the electronic structure of solids. Comparing their results and our calculations, we can conclude that LDA + SOC calculation yields the correct spin-orbit splitting and the most accurate positions of the 4f derived single-particle-like excitations [19].

There are three pieces of Fermi surface for YbRh<sub>2</sub>Si<sub>2</sub> from the LDA calculation, which is shown in figure 5. The FS splits into three different non-touching sheets. There are two tiny cylinder Fermi surfaces around the Z point in the top panel of figure 5 which is from the Rh 4d bands. And there are much larger Fermi surfaces at the boundary of the BZ with the form of a saucer and a butterfly, which are from the Ce 4f bands.

Density functional calculations are very reliable in calculating the instability to ferromagnetism. The presence of an electronic instability is signalled by a divergence of the corresponding susceptibility. In the following we study the uniform magnetic susceptibility using the method of Janak [20]. The uniform magnetic susceptibility of a metal can be written as

$$\chi = \frac{\chi_0}{1 - N(E_F)I}, \quad (1)$$

where the numerator stands for the Pauli susceptibility of a gas of non-interacting electrons proportional to the density of states at the Fermi level  $N(E_F)$ , and the denominator represents the enhancement due to electron-electron interaction. Within the Kohn-Sham formalism of density functional theory the Stoner parameter  $I$  is related to the second derivative of the exchange-correlation functional with respect to the magnetization density. We have evaluated, within the density functional theory formalism, the Stoner enhancement of the susceptibility  $\chi = \frac{\chi_0}{1 - IN(E_F)} \equiv S\chi_0$ , where  $\chi_0 = 2 \mu_B^2 N(E_F)$  is the non-interacting susceptibility and  $S$  gives the electron-electron enhancement in terms of the Stoner constant  $I$ . We have calculated  $I$  using both the Janak-Vosko-Perdew theory [20] and fixed spin moment calculations [21]. The calculated density of states and Stoner parameter  $I$  give  $IN(E_F) \sim 0.65$ , smaller than unity, which does not show a ferromagnetic instability.

A heavy fermion compound is characterized by a larger electronic specific heat coefficient  $\gamma$ . YbRh<sub>2</sub>Si<sub>2</sub> is a heavy fermion compound with  $\gamma = 1.7 \text{ J K}^{-2} \text{ mol}^{-1}$ . The large specific heat coefficient of the YbRh<sub>2</sub>Si<sub>2</sub> compound could not be yielded by our band calculation. This can be seen from the calculated electronic structure. It can be found that the total number of DOS at the Fermi level is about 3.10 states  $\text{eV}^{-1}$ , which corresponds to  $\gamma_b = 7.25 \text{ mJ K}^{-2} \text{ mol}^{-1}$  and underestimates the experimental value by a factor of 235. The discrepancy between the band calculation and experiment for the specific heat coefficient is attributed to the formation of a quasiparticle. There is an exchange interaction  $J$  between the local f and the conduction electrons in YbRh<sub>2</sub>Si<sub>2</sub>. The ground state of the Ce compound is determined by the competition of the Kondo and indirect RKKY interactions. With a large  $J$ , the Kondo coupling becomes strong and the system located at the borderline of the magnetic-nonmagnetic transition. The exchanging interaction between the local f electron and the conduction electrons will result in the formation of a quasiparticle. It has a larger mass compared with the bare electron and the enhancement of mass increases with increase of the exchange. Because of the volume contraction, the exchange interaction between the f and the conduction electrons is large in



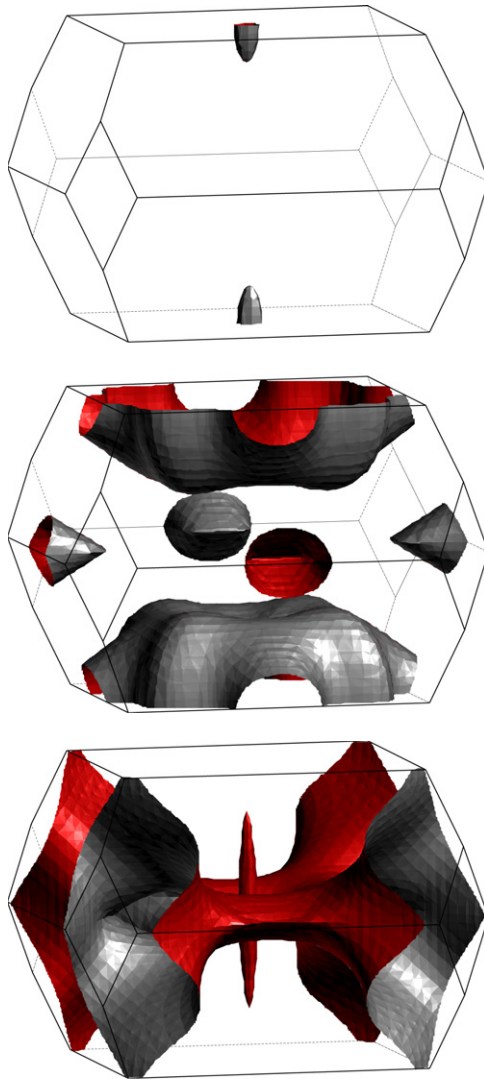


**Figure 5.** Fermi surfaces with LDA calculation (from the top, bands 48, 49, 50).

$\text{YbRh}_2\text{Si}_2$ . This will result in the  $f$  electrons behaving like itinerant electrons and the narrow  $f$  bands being located at the Fermi level. On the other hand, when the exchange interaction between  $f$  and conduction electrons is smaller, the occupied  $4f$  orbitals are located near the Fermi level while the unoccupied  $4f$  orbitals are at the conduction bands. The quasiparticle mass is appropriate to the number of DOS at the Fermi level. So the quasiparticle mass is substantially enhanced in  $\text{YbRh}_2\text{Si}_2$ . Indeed, it has been shown that when the Yb  $4f$  electrons in  $\text{YbRh}_2\text{Si}_2$  are treated as localized electrons, the quasiparticle mass is enhanced over the band calculation by a factor of 235.

## 5. Summary

In this work we studied the electronic band structure with three different schemes. In each case the  $4f$  bands are very flat and lie near the Fermi level. The band structure calculations indicate

that YbRh<sub>2</sub>Si<sub>2</sub> is a mixed-valence compound. This shows that the Coulomb potential on Yb 4f orbitals and the spin-orbit interaction are key factors for understanding the electronic and magnetic properties of YbRh<sub>2</sub>Si<sub>2</sub>. When the Coulomb potential is added to the Yb 4f orbitals, the degeneracy between the different f orbitals will be lifted and they are split into lower Hubbard bands at the Fermi level and unoccupied upper Hubbard bands in the conduction band. The exchange interaction between local f electrons and conduction electrons play an important role in their heavy fermion characters. And the fully relativistic band structure scheme shows that spin-orbit coupling splits the 4f states into two manifolds, the 4f<sub>7/2</sub> and the 4f<sub>5/2</sub> multiplets. The three different Fermi surfaces are made of the Rh 4d and Yb 4f states. The f electrons can be delocalized through the hybridization with conduction electrons. If there is no hybridization between f and conduction electrons, the f electron number becomes just an integer and the f electrons are localized. The almost localized f electrons and delocalized conduction electrons hybridize, making the f electron number deviate from an integer, and maintain the metallic state against the strong electron correlations between f electrons. Therefore the hybridization between f and conduction d electrons plays an important role in YbRh<sub>2</sub>Si<sub>2</sub>.

### Acknowledgments

We are grateful for illuminating discussions with H O Lee, C Geibel, P Genenwart, Z Fisk, R Martin and A J Freeman.

### References

- [1] Stewart G R 2001 *Rev. Mod. Phys.* **73** 797
- [2] Bogenberger B and von Lohneysen H 1995 *Phys. Rev. Lett.* **74** 1016
- [3] Grosche F M, Julian S R, Mathur N D and Lonzarich G G 1996 *Physica B* **223/224** 50
- [4] Walker I R, Grosche F M, Freye D M and Lonzarich G G 1997 *Physica C* **282–287** 303
- [5] Ishida K, MacLaughlin D E, Bernal O O, Heffner R H, Nieuwenhuys G J, Trovarelli O, Geibel C and Steglich F 2003 *Physica B* **326** 403
- [6] Trovarelli O, Geibel C, Mederle S, Langhammer C, Grosche F M, Gegenwart P, Lang M, Sparn G and Steglich F 2000 *Phys. Rev. Lett.* **85** 626
- [7] Gegenwart P, Custers J, Geibel C, Neumaier K, Tayama T, Tenya K, Trovarelli O and Steglich F 2002 *Phys. Rev. Lett.* **89** 056402
- [8] Trovarelli O, Custers J, Gegenwart P, Geibel C, Hinze P, Mederle S, Sparn G and Steglich F 2002 *Physica B* **312/313** 401
- [9] Custers J, Gegenwart P, Wilhelm H, Neumaler K, Tokiwa Y, Trovarelli O, Geibel C, Steglich F, Pepin C and Coleman P 2003 *Nature* **424** 524
- [10] Ishida K, Okamoto K, Kawasaki Y, Kitaoka Y, Trovarelli O, Geibel C and Steglich F 2002 *Phys. Rev. Lett.* **89** 107202
- [11] Norman M R 2005 *Phys. Rev. B* **71** 220405
- [12] Koepfner K and Eschrig H 1999 *Phys. Rev. B* **59** 1743  
Eschrig H 1989 *Optimized LCAO Method and the Electronic Structure of Extended Systems* (Berlin: Springer)
- [13] Perdew J P and Wang Y 1992 *Phys. Rev. B* **45** 13244
- [14] Liechtenstein A I, Anisimov V I and Zaanen J 1995 *Phys. Rev. B* **52** R5468  
Schik A B, Liechtenstein A I and Pickett W E 1999 *Phys. Rev. B* **60** 10728
- [15] Shick A B, Novikov D L and Freeman A J 1997 *Phys. Rev. B* **57** R14259
- [16] Tinkham M 2003 *Group Theory and Quantum Mechanics* (New York: Dover)
- [17] Schik A B, Pickett W E and Fadley C S 2000 *J. Appl. Phys.* **87** 5878
- [18] Kunes J, Ku W and Pickett W E 2005 *J. Phys. Soc. Japan* **74** 1408
- [19] Fisk Z *et al.*, unpublished
- [20] Janak J F 1977 *Phys. Rev. B* **16** 255  
Vosko S H and Perdew J P 1975 *Can. J. Phys.* **53** 1385
- [21] Schwarz K and Mohn P 1984 *J. Phys. F: Met. Phys.* **14** L129

## Erratum

### First-principles study of the electronic structure of heavy fermion $\text{YbRh}_2\text{Si}_2$

T Jeong 2006 *J. Phys.: Condens. Matter* **18** 6289–6297

The band structure in figure 2(b) and density of states in figure 3(b) for LDA +U calculation are incorrect and should be replaced by the new figures below. This change does not affect the conclusions of the paper. W E Pickett is removed from the list of authors.

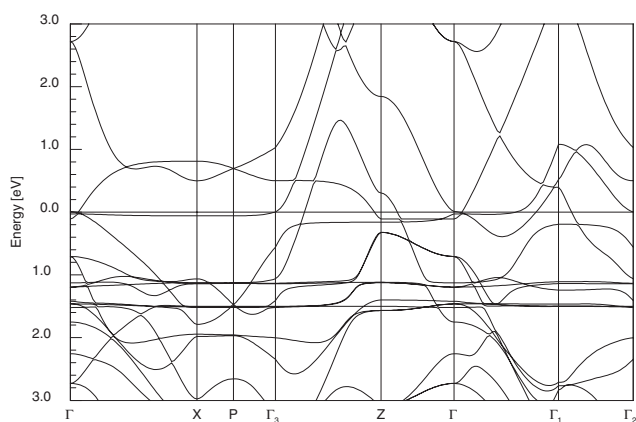


**Figure 2(b).** The band structure of  $\text{YbRh}_2\text{Si}_2$  for LDA+U calculation.

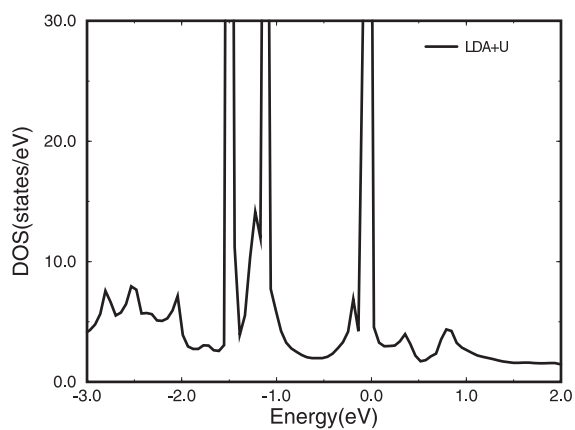


**Figure 3(b).** The density of states of  $\text{YbRh}_2\text{Si}_2$  for LDA+U calculation.